

**X-ray study of the crystal structure of  $\text{La}_{1-x}\text{Ba}_x\text{MnO}_3$** 

V. S. Gaviko\* and N. G. Bebenin

*Institute of Metal Physics, Ural Division, RAS, Kovalevskaya Street 18, Ekaterinburg 620041, Russia*

Ya. M. Mukovskii

*Moscow State Steel & Alloys Institute, Leninskii Prospekt 4, Moscow 117936, Russia*

(Received 27 April 2007; revised manuscript received 20 March 2008; published 10 June 2008)

The x-ray study of the crystal structure of  $\text{La}_{1-x}\text{Ba}_x\text{MnO}_3$  ( $0.14 \leq x \leq 0.25$ ) single crystal manganites has been performed at temperatures from 80 to 400 K. In all the crystals, the transition from the low-temperature orthorhombic  $Pnma$  phase to the high-temperature rhombohedral  $R\bar{3}c$  phase has been observed. In the  $x = 0.20$  and  $0.25$  manganites, the  $Pnma$  and  $R\bar{3}c$  phases coexist in the range of 20–30 K width while in the  $x = 0.14$  and  $0.15$  crystals, the mixture of the phases has been found in a range whose width exceeds 150 K. The  $Pnma$ - $R\bar{3}c$  transition heat and the change in the cell volume have been shown to be very small as compared to manganites.

DOI: [10.1103/PhysRevB.77.224105](https://doi.org/10.1103/PhysRevB.77.224105)

PACS number(s): 61.66.-f, 75.47.Lx

**I. INTRODUCTION**

The interest in the rare-earth manganites of general formula  $R_{1-x}D_x\text{MnO}_3$ , where  $R$  stands for a rare earth,  $D$  is a divalent ion, stems from the colossal magnetoresistance (CMR) observed near Curie temperature  $T_C$ .<sup>1,2</sup> A characteristic feature of the CMR materials is the strong interaction of charge carriers with crystal lattice. Unfortunately, even the room temperature data on the crystal structure of the CMR manganites published by various scientific groups can differ significantly. In particular, this is true for the  $\text{La}_{1-x}\text{Ba}_x\text{MnO}_3$  family. Thus the neutron-diffraction study of the vacancy-free La-Ba manganites by Dabrowski *et al.*<sup>3</sup> showed that the structure of the manganites was orthorhombic (space group  $Pbnm$ ) at  $x < 0.13$  and it was rhombohedral (space group  $R\bar{3}c$ ) at  $x > 0.13$ . Chaitali Roy and R. C. Budhani found that in the compositions with  $0 < x \leq 0.25$ , a single phase rhombohedral compound of decreasing rhombicity was formed while at  $0.25 < x < 0.4$  there was the ideal cubic perovskite structure.<sup>4</sup> H.L. Ju *et al.*<sup>5</sup> reported that the crystal structure changed from tetragonal for  $0 < x < 0.13$  to rhombohedral for  $0.13 < x < 0.38$ , then to cubic for  $0.38 < x < 0.5$ . According to Trukhanov *et al.*<sup>6</sup> the lattice of the perovskites is orthorhombic at the Ba content of  $0 < x < 0.05$ , rhombohedral if  $0.10 < x < 0.25$  and cubic at  $0.27 < x < 0.50$ .

There are a few articles dealing with the temperature dependence of the crystal structure of  $\text{La}_{1-x}\text{Ba}_x\text{MnO}_3$ . The first work was seemingly published by Radaelli *et al.*<sup>7</sup> who found that the lattice of  $\text{La}_{0.70}\text{Ba}_{0.30}\text{MnO}_3$  was orthorhombic (space group  $Imma$ ) at  $T < 150$  K and rhombohedral ( $R\bar{3}c$ ) at  $T > 200$  K. The unit cell volume  $3V$  was found to be a monotone function of temperature and the  $Imma$ - $R\bar{3}c$  phase transition was not seen on the  $V(T)$  curve. Mandal and Ghosh<sup>8</sup> studied the La-Ba single crystals with  $x = 0.125$ ,  $0.15$  and  $0.20$ . They found the orthorhombic  $Pbnm$  and the rhombohedral  $R\bar{3}c$  phases with the  $Pbnm$ - $R\bar{3}c$  transition temperature decreasing with increasing Ba content  $x$ . The study of  $\text{La}_{2/3}\text{Ba}_{1/3}\text{MnO}_3$  made by Beznosov *et al.*<sup>9</sup> revealed the coexistence of the low-temperature  $Imma$  and the high-

temperature  $R\bar{3}c$  phases in a wide temperature range with the  $Imma$ - $R\bar{3}c$  transition taking place around 200 K. Recently it was stated that the low-temperature phase of  $\text{La}_{0.815}\text{Ba}_{0.185}\text{MnO}_3$  single crystal was monoclinic rather than orthorhombic and the structural transformation to  $R\bar{3}c$  phase occurs at  $T = 187$  K.<sup>10</sup> A weak change of the slope was found of the temperature dependence of the unit cell volume that occurs at  $\approx 256$  K near the Curie temperature  $T_C = 251$  K. In our early study<sup>11</sup> of  $\text{La}_{0.8}\text{Ba}_{0.2}\text{MnO}_3$  single crystal, the  $Pbnm$ - $R\bar{3}c$  transition was found to occur around 190 K with the two phases coexisting at least in the range of  $185 < T < 196$  K.

One can see that the data on the lattice structure of the  $\text{La}_{1-x}\text{Ba}_x\text{MnO}_3$  remain contradictory. In view of this, we have carried out a systematic study of the crystal structure of the ferromagnetic La-Ba single crystals with  $x = 0.14$ ,  $0.15$ ,  $0.20$  and  $0.25$ . Special attention has been paid to the vicinity of the structural transition where different crystalline phases coexist. Since the limiting Ba concentration for perovskite phase formation is close to 0.3, see Ref. 12, our set of the single crystals cover almost the entire concentration range in which the CMR effect is observed.

**II. EXPERIMENT**

The single crystals of  $\text{La}_{1-x}\text{Ba}_x\text{MnO}_3$  were grown by the floating-zone method; the details have been published elsewhere.<sup>12</sup> The powder samples for the diffractometer were prepared by grinding the crystals; the typical size of particles was 30–60  $\mu\text{m}$ . The crystal structure was studied with DRON-6 diffractometer. The room temperature measurements were made in Cr radiation. The temperature dependence of x-ray patterns was investigated over the range 80–400 K in Fe radiation under warming. The structural parameters were obtained by Rietveld refinement using the FULLPROF software.<sup>13</sup>

**III. CRYSTAL STRUCTURE AT ROOM TEMPERATURE**

Figure 1 shows the experimental x-ray patterns (circles) and calculated ones (solid lines) of the  $x = 0.25$  manganites;

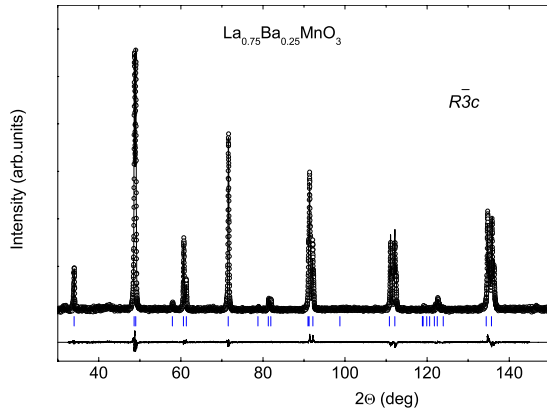


FIG. 1. (Color online) Observed (circles) and calculated (line) x-ray diffraction pattern for the  $x=0.25$  sample ( $T=300$  K). The Bragg-peak positions are shown for  $R\bar{3}c$  structure.

the results for the  $x=0.20$  sample are similar (see Ref. 11). Only the lines of rhombohedral  $R\bar{3}c$  phase are observed. On the contrary, the samples with lower Ba contents turn out to be in two phase state at room temperature. Figure 2 shows the x-ray pattern for the  $x=0.14$  sample. The experimental curve can be very well described in terms of mixture of the rhombohedral  $R\bar{3}c$  phase and orthorhombic  $Pnma$  phase (from now on, we shall use the  $Pnma$  setting, which is more common at present for space group No. 62, instead of  $Pbmn$  setting used in early publications). In Fig. 3 we show some peaks in detail. The volume of the  $Pnma$  phase is equal approximately to 40% and 60% in the  $x=0.15$  and  $x=0.14$  samples, respectively, i.e., it increases with decreasing Ba content.

In Table I, we present the calculated lattice parameters and unit cell volume (per formula unit). It is interesting that in the two phase samples ( $x=0.14$  and  $x=0.15$ ), the volumes of  $R\bar{3}c$  and  $Pnma$  phases are very close to each other, the volume of the orthorhombic phase being slightly greater than that of the rhombohedral one.

In Fig. 4 we show the room temperature rhombohedral phase parameters as a function of Ba content  $x$  obtained by

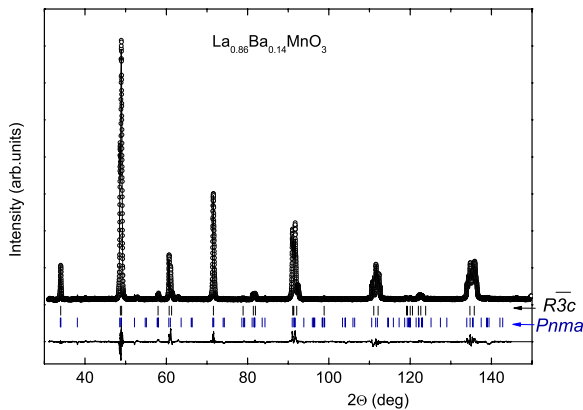


FIG. 2. (Color online) Observed (circles) and calculated (line) x-ray diffraction pattern for the  $\text{La}_{0.86}\text{Ba}_{0.14}\text{MnO}_3$  sample ( $T=300$  K). The Bragg-peak positions are shown for  $R\bar{3}c$  and  $Pnma$  structures.

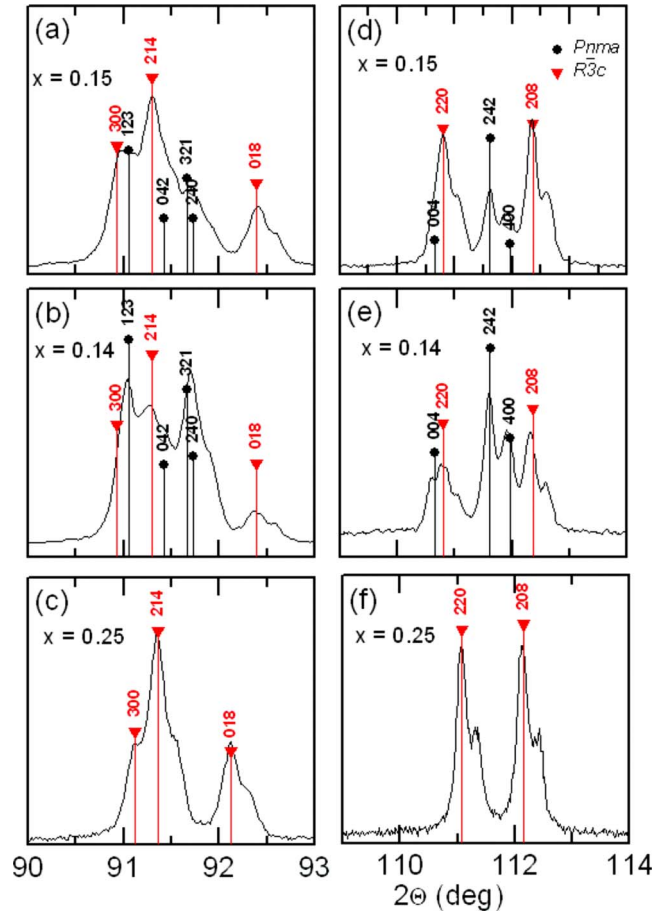


FIG. 3. (Color online) The structure of some diffraction peaks for the  $x=0.15$ ,  $x=0.14$  and  $x=0.25$  samples.

us and reported in Refs. 3, 6, and 10. As  $x$  increases, the parameter  $c$  increases as well while the parameter  $a$  and the cell volume decrease. The concentration dependence of the lattice parameters in  $\text{La}_{1-x}\text{Ba}_x\text{MnO}_3$  is very similar to that observed earlier in  $\text{La}_{1-x}\text{Sr}_x\text{MnO}_3$  single crystals in which the increase in Sr content also results in the reduction of the volume.<sup>13</sup> This reduction in  $\text{La}_{1-x}\text{Ba}_x\text{MnO}_3$  and  $\text{La}_{1-x}\text{Sr}_x\text{MnO}_3$  is due to the appearance of  $\text{Mn}^{4+}$  ions whose radius is less than that of  $\text{Mn}^{3+}$ . In the La-Ba manganites, however, the dependence of the volume on  $x$  is much weaker than in  $\text{La}_{1-x}\text{Sr}_x\text{MnO}_3$  because the radius of  $\text{Ba}^{2+}$  is significantly greater than that of  $\text{Sr}^{2+}$ , which partly compensates for the effect of the appearance of  $\text{Mn}^{4+}$  on the crystal lattice parameters.

Comparing the data obtained in this work with the data reported by other authors, we see that our data as well as the data for the  $\text{La}_{0.815}\text{Ba}_{0.185}\text{MnO}_3$  single crystal<sup>10</sup> are closest to those reported in Ref. 3. It is important that Dabrowski *et al.*<sup>3</sup> prepared and studied the polycrystalline samples of  $\text{La}_{1-x}\text{Ba}_x\text{MnO}_3$  which were vacancy-free. Therefore we may believe that the chemical composition of our single crystals is close to nominal one. On the other hand, the appearance of the oxygen vacancies is known to result in the increase of the lattice parameters and the cell volume in the manganites of  $\text{La}_{1-x}\text{D}_x\text{MnO}_3$  with  $\text{D}=\text{CaSr}, \text{Ba}$ .<sup>6,14,15</sup> The fact that the lattice parameters reported in Ref. 6 are noticeably greater than

TABLE I. Lattice parameters of  $\text{La}_{1-x}\text{Ba}_x\text{MnO}_3$  at the room temperature

	$x=0.14$		$x=0.15$		$x=0.20$	$x=0.25$
	$Pnma$	$R\bar{3}c$	$Pnma$	$R\bar{3}c$	$R\bar{3}c$	$R\bar{3}c$
$a$ (Å)	5.5240(2)	5.5631(2)	5.5265(2)	5.5637(2)	5.5525(1)	5.5513(1)
$b$ (Å)	7.8124(2)		7.8122(3)			
$c$ (Å)	5.5692(2)	13.4461(3)	5.5684(2)	13.4399(2)	13.4531(2)	13.4753(2)
$V$ (per formula unit, Å <sup>3</sup> )	60.09	60.06	60.10	60.05	59.87	59.94

those reported by Dabrowski *et al.*<sup>3</sup> can be an evidence for the oxygen vacancies to exist even in the nominally stoichiometric samples of the La-Ba manganites studied in Ref. 6.

IV. EVOLUTION OF CRYSTAL STRUCTURE WITH TEMPERATURE

When temperature is decreased, the  $R\bar{3}c$ - $Pnma$  structural transition occurs in all the La-Ba manganites. Figures 5 and

6 show the temperature dependences of the lattice parameters and the unit cell volume for the  $\text{La}_{0.75}\text{Ba}_{0.25}\text{MnO}_3$  and  $\text{La}_{0.86}\text{Ba}_{0.14}\text{MnO}_3$  manganites, respectively. The curves are similar to those reported for  $\text{La}_{0.80}\text{Ba}_{0.20}\text{MnO}_3$  crystal<sup>11,16</sup> and  $\text{La}_{1-x}\text{Sr}_x\text{MnO}_3$  with  $x \leq 0.2$ .<sup>17,18</sup> All the La-Ba crystals undergo the first order  $R\bar{3}c$ - $Pnma$  transition while the La-Sr manganites with  $x \geq 0.25$  are always in the rhombohedral phase. Near the structural transition temperature  $T_S$ , there is a mixture of the  $R\bar{3}c$  and  $Pnma$  phases. In  $\text{La}_{0.75}\text{Ba}_{0.25}\text{MnO}_3$  and  $\text{La}_{0.80}\text{Ba}_{0.20}\text{MnO}_3$ , the width of range in which the coexistence of the phases is observed is about 15–20 K while in the  $x=0.14$  and  $x=0.15$  crystals, it exceeds 100 K; see Fig. 6.

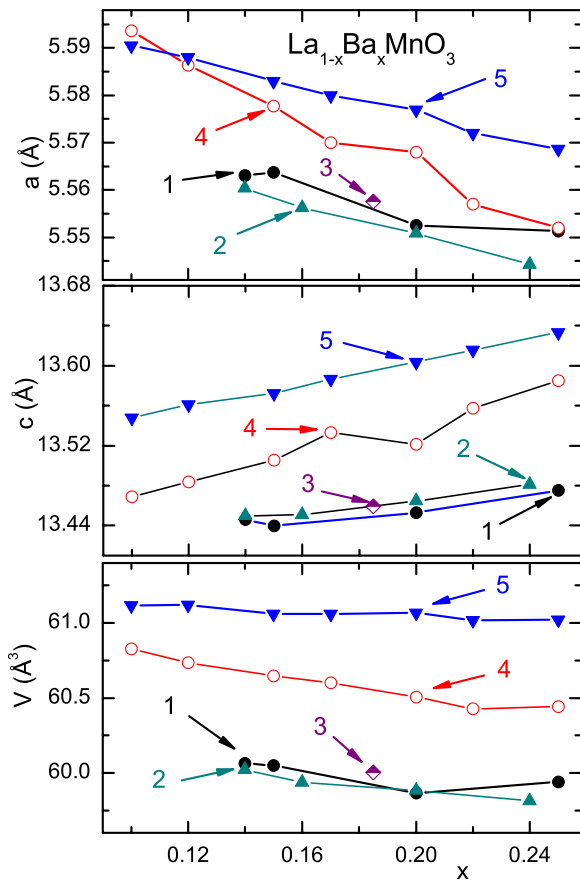


FIG. 4. (Color online) Lattice parameters for  $\text{La}_{1-x}\text{Ba}_x\text{MnO}_3$  at the room temperature: 1—single crystals studied in this work; 2—vacancy-free polycrystals studied by Dabrowski *et al.* (Ref. 3); 3— $\text{La}_{0.815}\text{Ba}_{0.185}\text{MnO}_3$  single crystal (Ref. 10); 4—(nominally) stoichiometric polycrystalline samples of  $\text{La}_{1-x}\text{Ba}_x\text{MnO}_3$  investigated by Trukhanov *et al.* (Ref. 6); 5—the anion-deficient polycrystalline samples of  $\text{La}_{1-x}\text{Ba}_x\text{MnO}_{3-x/2}$  reported by Trukhanov *et al.* (Ref. 6).

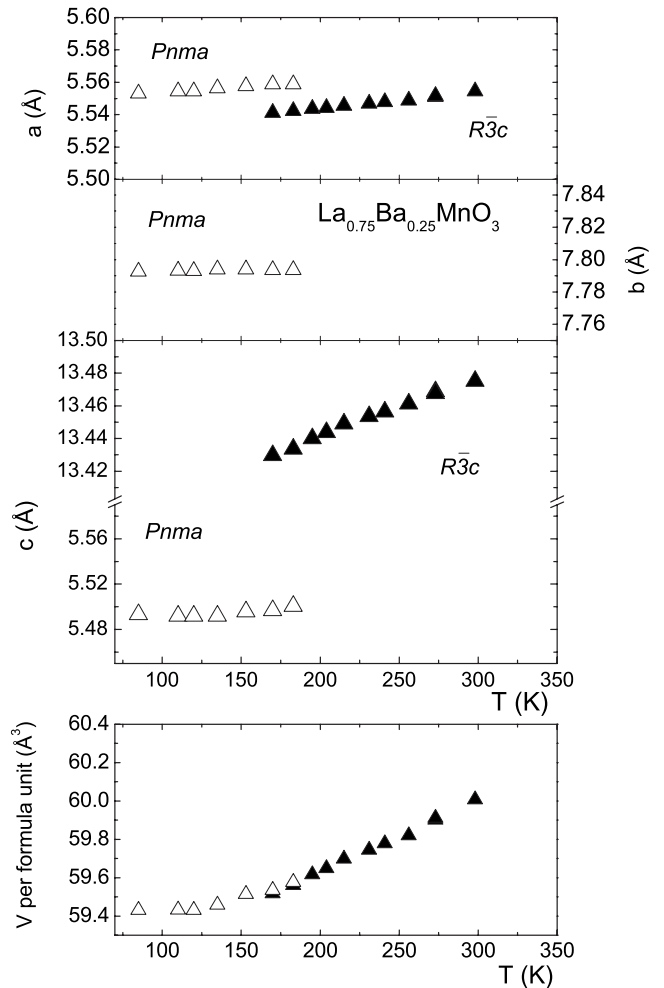


FIG. 5. Lattice parameters of  $\text{La}_{0.75}\text{Ba}_{0.25}\text{MnO}_3$  as a function of temperature.

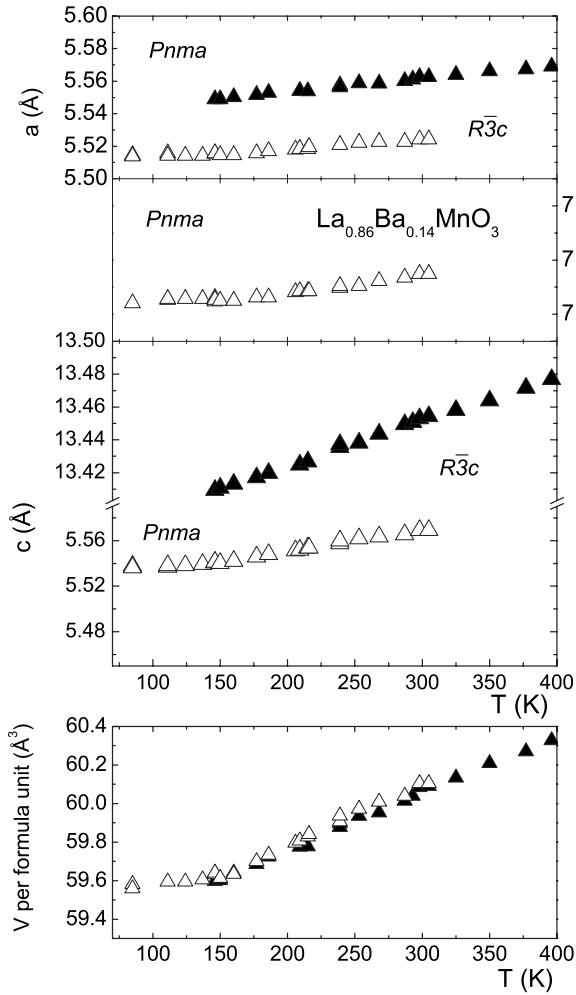


FIG. 6. Temperature dependence of lattice parameters of  $\text{La}_{0.86}\text{Ba}_{0.14}\text{MnO}_3$ .

The change in the volume  $\Delta V = V^{R\bar{3}c} - V^{Pnma}$  under the structural transition is essentially less in  $\text{La}_{1-x}\text{Ba}_x\text{MnO}_3$  than in  $\text{La}_{1-x}\text{Sr}_x\text{MnO}_3$  where the value of  $\Delta V$  is of order  $0.1\text{--}0.2 \text{ \AA}^3$  per formula unit, the volume of the  $Pnma$  phase being greater than that of  $R\bar{3}c$  phase. In fact, the  $\Delta V$  values derived from our x-ray measurements are within the experimental error. It is possible, however, to estimate  $\Delta V$  in  $\text{La}_{0.80}\text{Ba}_{0.20}\text{MnO}_3$  by making use of the data published in Refs. 11 and 19. In the  $x=0.20$  crystal, the application of hydrostatic pressure  $P$  produces a huge downward shift of  $T_S$  ( $dT_S/dP \approx -3 \text{ K/kbar}$ ) indicating that the  $R\bar{3}c$  phase is stabilized under pressure.<sup>20</sup> This implies that the volume of the  $R\bar{3}c$  phase is less than that of the  $Pnma$  phase. The transition temperature  $T_S(P, H)$  obeys the Clapeyron equations:

$$\frac{dT_S}{dP} = \frac{T_S \Delta V}{q}, \quad H = \text{const}, \quad (1)$$

$$\frac{dT_S}{dH} = -\frac{T_S \Delta M}{q}, \quad P = \text{const}, \quad (2)$$

where  $H$  is magnetic field,  $\Delta M = M^{R\bar{3}c} - M^{Pnma}$ ,  $M$  stands for magnetization. According to Refs. 11 and 20,  $T_S \approx 190 \text{ K}$ ,

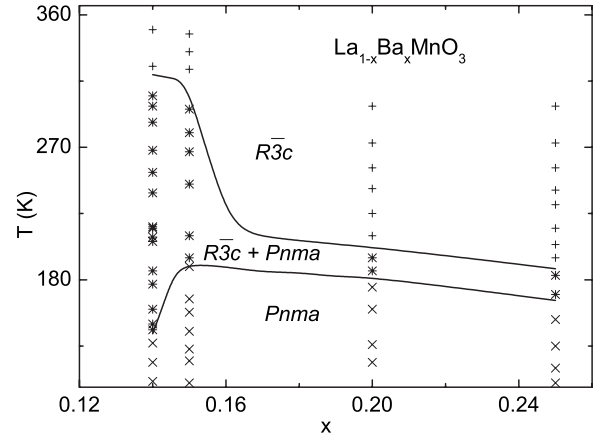


FIG. 7.  $T$ - $x$  phase diagram for the  $\text{La}_{1-x}\text{Ba}_x\text{MnO}_3$  manganites.  $Pnma$  phase ( $\times$ );  $R\bar{3}c$  phase ( $+$ ); mixture of the  $Pnma$  and  $R\bar{3}c$  phases ( $*$ ). Notice that there is a wide region of coexistence of  $Pnma$  and  $R\bar{3}c$  phases.

$\Delta M \approx 4 \text{ G}$ ,  $dT_S/dH \approx 4.5 \cdot 10^{-5} \text{ K/Oe}$ , so that from Eq. (2) we obtain  $q \approx 0.06 \text{ kJ/mol}$ . The transition heat in  $\text{La}_{0.80}\text{Ba}_{0.20}\text{MnO}_3$  is significantly less than in  $\text{La}_{0.80}\text{Sr}_{0.20}\text{MnO}_3$  in which it is around  $0.2 \text{ kJ/mol}$ .<sup>20</sup> Making use of Eq. (1) and the  $dT_S/dP$  value given above, we immediately obtain  $\Delta V \approx -0.02 \text{ \AA}^3$  per formula unit. This value of  $\Delta V$  agrees with the values that follow from the data given in Table I. Apparently, the very small  $\Delta V$  favor the coexistence of the orthorhombic and rhombohedral phases.

From information obtained in this work, we have constructed the structural phase diagram of  $\text{La}_{1-x}\text{Ba}_x\text{MnO}_3$  shown in Fig. 7. Stars in Fig. 7 denote the mixture of the  $Pnma$  and  $R\bar{3}c$  phases. One can see that the mixed-phase region widens as the Ba content  $x$  decreases. The reason why the region of coexisting of the orthorhombic and rhombohedral phases is so wide in the  $x=0.14$  and  $0.15$  manganites remains unclear.

The wide range of the coexistence in the low doped La-Ba manganites agrees with the results of ultrasound measurements, which have revealed the giant thermal hysteresis of longitudinal sound velocity  $V_l$  and internal friction  $Q^{-1}$  connected with the structural transition.<sup>21,22</sup> The hysteretic behavior of  $V_l$  and  $Q^{-1}$  in the range of  $100\text{--}200 \text{ K}$  width was reported also for the  $x=0.20$  and  $x=0.25$  manganites although the x-ray measurements reveal the coexistence of the two crystal structures in the significantly narrower temperature interval. The reason is that there is a great (about 20%) difference between the sound velocities in the  $Pnma$  and  $R\bar{3}c$  phases, so that  $V_l$  is extremely sensitive to the  $Pnma$  inclusions in the  $R\bar{3}c$  matrix and vice versa.

The resistivity measurements<sup>11,22–24</sup> have revealed the thermal hysteresis in the range of  $20\text{--}30 \text{ K}$  width in all the La-Ba manganites. The difference between the resistivity values taken at heating and cooling run is, however, very small (1% or less) even in a close vicinity of  $T_S$ ; the hysteresis is more pronounced in the  $\text{La}_{0.80}\text{Ba}_{0.20}\text{MnO}_3$  crystal in which  $T_S$  is not too far from the Curie temperature ( $T_C = 252 \text{ K}$ ). It follows that at  $T_S \ll T_C$  or  $T_S \gg T_C$ , the electronic density of states is almost the same in the  $Pnma$  and  $R\bar{3}c$

phases; the structural transition influences the electronic transport mainly through the change in the magnetic subsystem.

## V. CONCLUSION

The x-ray study of the crystal structure of single crystals of  $\text{La}_{1-x}\text{Ba}_x\text{MnO}_3$  manganites ( $x=0.14, 0.15, 0.20, \text{ and } 0.25$ ) has been performed over temperature range of 80–400 K. The low-temperature orthorhombic  $Pnma$  and the high-temperature rhombohedral  $R\bar{3}c$  phases have been observed. At the room temperature, the lattice parameters of all the samples are very close to the parameters reported by Dabrowski *et al.*<sup>3</sup> for the polycrystalline vacancy-free samples of

La-Ba manganites. In the  $x=0.14$  and  $x=0.15$  samples, the mixture of the  $Pnma$  and  $R\bar{3}c$  phases is observable in a wide (100 K or more) temperature range compared to the  $\sim 20$  K range in the  $x=0.20$  and  $x=0.25$  samples. The  $Pnma$ - $R\bar{3}c$  transition heat is about  $q \approx 0.06$  kJ/mol. The  $R\bar{3}c$ - $Pnma$  transition results in the very small change in the volume, which favors the coexistence of the phases of different symmetry.

## ACKNOWLEDGMENTS

This work was supported by RFBR Grant No. 03-02-16065.

\*Corresponding author.

FAX: +7-343-3745244. gaviko@imp.uran.ru

<sup>1</sup>M. B. Salamon and M. Jaime, *Rev. Mod. Phys.* **73**, 583 (2001).

<sup>2</sup>E. Dagotto, *Nanoscale Phase Separation and Colossal Magnetoresistance: The Physics of Manganites and Related Compounds* (Springer-Verlag, Berlin, 2002).

<sup>3</sup>B. Dabrowski, K. Rogacki, X. Xiong, P. W. Klamut, R. Dybziński, J. Shaffer, and J. D. Jorgensen, *Phys. Rev. B* **58**, 2716 (1998).

<sup>4</sup>Chaitali Roy, R. C. Budhani, *J. Appl. Phys.* **85**, 3124 (1999).

<sup>5</sup>H. L. Ju, Y. S. Nam, J. E. Lee, and H. S. Shin, *J. Magn. Magn. Mater.* **219**, 1 (2000).

<sup>6</sup>S. V. Trukhanov, L. S. Lobanovskii, M. V. Bushinsky, I. O. Troyanchuk, and H. Szymczak, *J. Phys.: Condens. Matter* **15**, 1783 (2003).

<sup>7</sup>P. G. Radaelli, M. Marezio, H. Y. Hwang, and S.-W. Cheong, *J. Solid State Chem.* **122**, 144 (1996).

<sup>8</sup>P. Mandal and B. Ghosh, *Phys. Rev. B* **68**, 014422 (2003).

<sup>9</sup>A. B. Beznosov, V. A. Desnenko, E. L. Fertman, C. Ritter, and D. D. Khalyavin, *Phys. Rev. B* **68**, 054109 (2003).

<sup>10</sup>Nicola Rotiroli, Sander van Smaalen, Rafael Tamazyan, and Ya. Mukovskii, *Phys. Rev. B* **74**, 104423 (2006).

<sup>11</sup>V. E. Arkhipov, N. G. Bebenin, V. P. Dyakina, V. S. Gaviko, A. V. Korolev, V. V. Mashkautsan, E. A. Neifeld, R. I. Zainullina, Ya. M. Mukovskii, and D. A. Shulyatev, *Phys. Rev. B* **61**, 11229 (2000).

<sup>12</sup>D. Shulyatev, N. Kozlovskaya, R. Privezentsev, A. Pestun, Ya. Mukovskii, L. Elochina, and S. Zverkov, *J. Cryst. Growth* **291**, 262 (2006).

<sup>13</sup>J. Rodrigues-Carvajal, FULLPROF, Version 3.20, December 2005.

<sup>14</sup>S. V. Trukhanov, N. V. Kasper, I. O. Troyanchuk, M. Tovar, H. Szymczak, and K. Bärner, *J. Solid State Chem.* **169**, 85 (2002).

<sup>15</sup>A. M. De León-Guevara, P. Berthet, J. Berthon, F. Millot, A. Revcolevschi, A. Anane, C. Dupas, K. Le Dang, J. P. Renard, and P. Veillet, *Phys. Rev. B* **56**, 6031 (1997).

<sup>16</sup>Ya. Mukovskii, V. Arkhipov, A. Arsenov, N. Bebenin, V. Dyakina, V. Gaviko, A. Korolev, S. Karabashev, V. Mashkautsan, E. Neifeld, D. Shulyatev, and R. Zainullina, *J. Alloys Compd.* **326**, 108 (2001).

<sup>17</sup>B. Dabrowski, X. Xiong, Z. Bukowski, R. Dybziński, P. W. Klamut, J. E. Siewenie, O. Chmaissem, J. Shaffer, C. W. Kimball, J. D. Jorgensen, and S. Short, *Phys. Rev. B* **60**, 7006 (1999).

<sup>18</sup>V. Gaviko, A. Korolev, V. Arkhipov, N. Bebenin, and Ya. Mukovskii, *Phys. Solid State* **47**, 1299 (2005).

<sup>19</sup>V. Laukhin, B. Martínez, J. Fontcuberta, and Y. M. Mukovskii, *Phys. Rev. B* **63**, 214417 (2001).

<sup>20</sup>E. A. Neifeld, N. G. Bebenin, V. E. Arkhipov, K. M. Demchuk, V. S. Gaviko, A. V. Korolev, N. A. Ugryumova, and Ya. M. Mukovskii, *J. Magn. Magn. Mater.* **295**, 77 (2005).

<sup>21</sup>R. I. Zainullina, N. G. Bebenin, A. M. Burkhanov, V. V. Ustinov, and Ya. M. Mukovskii, *J. Alloys Compd.* **394**, 39 (2005).

<sup>22</sup>R. I. Zainullina, N. G. Bebenin, V. V. Mashkautsan, V. V. Ustinov, and Ya. M. Mukovskii, *J. Magn. Magn. Mater.* **300**, e137 (2006).

<sup>23</sup>N. G. Bebenin, R. I. Zainullina, N. S. Chusheva, V. V. Ustinov, and Ya. M. Mukovskii, *J. Phys.: Condens. Matter* **17**, 5433 (2005).

<sup>24</sup>R. Zainullina, N. Bebenin, V. Mashkautsan, V. Ustinov, Ya. Mukovski, and A. Arsenov, *Phys. Solid State* **45**, 1754 (2003).